Helmholtz-Zentrum Dresden-Rossendorf (HZDR)

HELMHOLTZ ZENTRUM
DRESDEN ROSSENDORF

99mTechnetium-based Small Molecule Radiopharmaceuticals and Radiotracers Targeting Inflammation and Infection

Kniess, T.; Laube, M.; Wüst, F.; Pietzsch, J.;

Originally published:

October 2017

Dalton Transactions 46(2017), 14435-14451

DOI: https://doi.org/10.1039/c7dt01735a

Perma-Link to Publication Repository of HZDR:

https://www.hzdr.de/publications/Publ-25537

Release of the secondary publication
on the basis of the German Copyright Law § 38 Section 4.

^{99m}Technetium-based Small Molecule Radiopharmaceuticals and Radiotracers targeting Inflammation and Infection

Torsten Kniess[1], Markus Laube[1], and **Jens Pietzsch[1,2]**

[1]*Helmholtz-Zentrum Dresden-Rossendorf, Institute of Radiopharmaceutical Cancer Research, 01328 Dresden, Germany*

[2]*Technische Universität Dresden, Department of Chemistry and Food Chemistry, 01062 Dresden, Germany*

Abstract

In nuclear medicine the detection of inflamed and infected lesions is of growing interest and extensive efforts have been made to develop radiopharmaceuticals specific for inflammation or rather for discrimination of sterile inflammation from infection. ^{99m}Tc is the worldwide most-used radioisotope for SPECT investigations; the scope of this review article is to give an overview on the development of ^{99m}Tc-labeled small molecule radiotracers targeting inflammatory and infected lesions, from their radiopharmacological evaluation up to examples of clinical application. A systematic overview of ^{99m}Tc-citrate, ^{99m}Tc-antibiotics and antifungal agents as well as ^{99m}Tc-labeled antimicrobial peptides is provided. Additionally, the class of ^{99m}Tc-labeled cyclooxygenase-2 inhibitors is discussed, since cyclooxygenases are known to play a key role in inflammatory but also in malignant neoplastic diseases.

Introduction

Inflammation is a highly complex molecular and cellular tissue reaction that is triggered by various external and internal conditions like physical injury, exposure to chemical agents, ionizing radiation and biotic factors. Furthermore, inflammation is caused by certain disorders, resulting in attraction and accumulation of activated inflammatory cells and the action of panoply of extra- and intracellular molecules in the tissue stroma and epithelium. If biotic factors like viruses or bacteria are involved, inflammation evolves to be the key process of innate immune response against the infection.

In general, the associated heterogeneous clinical conditions may be classified in sterile or infectious acute inflammation and chronic inflammation, respectively.

Acute inflammation is characterized by local reddening, swelling, hyperthermia, pain and dysfunction, and is an early or immediate response to the injuring agent. Resolution of acute inflammation is accompanied by removal of the stimulus and by healing of the injured tissue, mostly resulting in complete restoration of the normal situation. The signs and symptoms of acute inflammation fade within several days. In contrast, chronic inflammation is a process lasting for weeks or months and is often associated by dysregulation of inflammatory cells and mediators,

triggering a self-sustaining response to injury, which finally often is accompanied by loss of function of the affected tissues in a local and sometimes systemic manner.

The origins of chronic inflammation are manifold. Prominent examples of clinical relevance are *i)* abdominal inflammation related to, e.g., appendicitis, pancreatitis, ulcerative colitis and Crohn's disease, *ii)* pulmonary inflammation related to, e.g., chronic obstructive pulmonary disease, sarcoidosis, recurrent pneumonia and tuberculosis, and *iii)* skeletal inflammation, related to, e.g., juvenile idiopathic arthritis, rheumatoid arthritis, osteomyelitis, and infected bone prostheses.[1]

Both sterile and infectious inflammatory states can be localized in one specific tissue or organ, or systemically can affect multiple sites. Current clinical challenges are *i)* the exact localization and functional characterization of inflammatory lesions, *ii)* the differentiation between sterile inflammation and infection, *iii)* the differentiation of inflammatory processes from other disease-related phenomena, *iv)* the identification of the molecular and cellular signature characterizing definite processes and diseases, *v)* the discrimination of adverse processes from normal wound healing, and *vi)* the monitoring of response and adverse effects related to certain therapeutic interventions.

A number of non-invasive diagnostic imaging tools are available for detection of inflamed and infected areas, e.g., ultrasonography (US), optical imaging (OI), computed tomography (CT) or magnetic resonance imaging (MRI).[2,3,4,5] Even though having excellent spatial resolution, these techniques are showing solely morphological changes and as a consequence abnormalities may often only be detected at later stages of the disease. Furthermore, in patients with metal orthopedic implants the application of MRI is excluded. Radioisotope based imaging procedures can provide useful information on physiologic and metabolic changes over the time, a radiolabeled probe capable of accumulating in the inflammatory lesion or site of infection would allow a specific diagnosis and a more targeted therapy for the individual patient. For that reason the search for radiolabeled agents targeting infection and inflammation was one of the first urgent needs in nuclear medicine based diagnosis and albeit a number of radiotracers suitable for single-photon emission computed tomography (SPECT) and later on positron emission tomography (PET) have been introduced, the ideal radiopharmaceutical for functional imaging of inflammation and/or infection still has not been found.

In the past, numerous radiotracers to identify infections and inflammatory lesions with SPECT and PET have been introduced. For reviews covering more radionuclides than ^{99m}Tc, the reader is referred to a number of comprehensive and excellent articles.[1,6,7,8,9,10,11] Radiotracers for imaging of inflammatory and infectious lesions are conventionally classified according to their mechanism of

action, showing non-specific and specific accumulation. (Figure 1) Non-specific radiopharmaceuticals are entering the inflamed areas due to enhanced vascular permeability and increased movement of white blood cells to the inflamed tissue (leucocyte extravasation). Specific processes of accumulation comprise target specific cellular migration (leucocyte transport), receptor binding or antibody-antigen based binding of the radiopharmaceutical to the inflamed/infected target.[1,8]

The accumulation of 2-[^{18}F]fluoro-desoxyglucose (**[^{18}F]FDG**) in cells with enhanced glucose metabolism is a specific process, however since this interaction is not only restricted to inflamed or infected targets and also includes e.g. cancer cells, [^{18}F]FDG is considered for inflammatory processes rather unspecific and hence resembles an intermediate as indicated in Figure 1. The role of [^{18}F]FDG and other PET radiotracers in infectious and inflammatory diseases is highlighted in additional review articles and is beyond the scope of this work. [12,13,14,15]

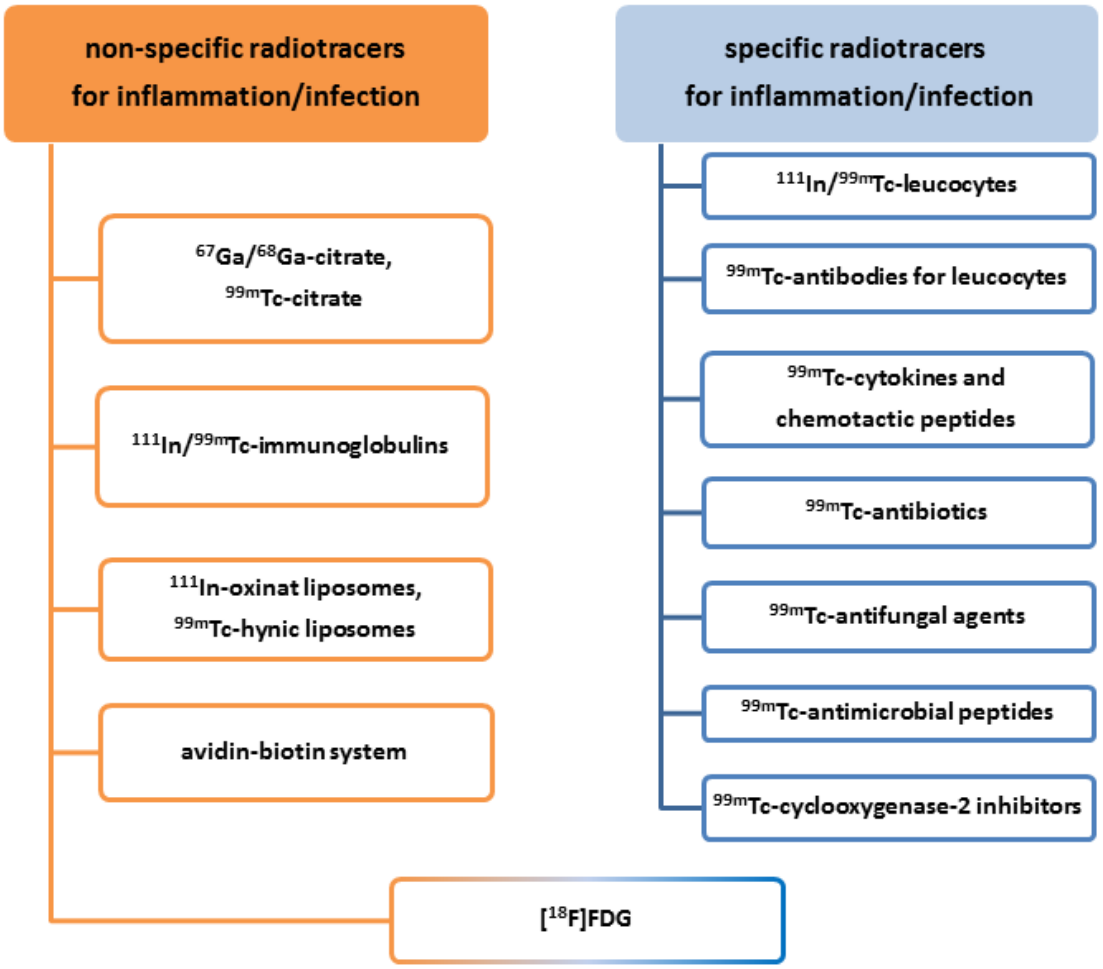

Figure 1. Radiopharmaceuticals for imaging inflammation and infection

^{99m}Technetium is the worldwide most used radionuclide with about 76.000 scans per day, covering approximately 85 % of all investigations in nuclear medicine.[16] The easily amenable ^{99}Mo generator

based production which is more or less throughout available, comfortable half-life (6 h), and convenient γ energy of 140 keV makes it the ideal radioisotope for SPECT investigations. As visible in Figure 1 ^{99m}Tc is an indispensable isotope for development of inflammation and infection targeting radiotracers and, rather than providing a complete listing, the focus of this review is to give an overview on a number of small molecule based ^{99m}Tc-complexes like ^{99m}Tc-citrate, ^{99m}Tc-labeled antibiotics, antifungals and antimicrobial peptides. In addition, recent outcomes in the development of ^{99m}Tc-labeled cyclooxygenase-2 (COX-2) inhibitors are highlighted.

^{99m}Tc-citrate

Citrate has turned out to be a suitable counter ion for cationic radiometals as ^{67}Ga or ^{99m}Tc according to its high *in vivo* compatibility and pharmacological innocuousness. Scintigraphic imaging with **^{67}Ga-citrate** has been performed since the 1970s [17,18] and since that time this radiotracer has emerged as a standard for detection of acute and chronic inflammation.[8,1] *In vivo* the ^{67}Ga-citrate dissociates from citrate and the [^{67}Ga]Ga^{3+} cation forms a complex with transferrin, the iron-binding protein in blood. As inflamed/infected tissue shows a slightly declined pH in comparison to normal blood pH, the ^{67}Ga transferrin dissociates in the inflamed area and ^{67}Ga binds to other proteins as a more stable complex. However, ^{67}Ga has some drawbacks like the need for a cyclotron due to production via ^{68}Zn(p,2n)^{67}Ga nuclear reaction, the long physical half-life of 3.26 d causing high radiation burden for patients, and the poor image quality and resolution according to the different electron and photon emission decay products. With the facile availability of generator produced ^{68}Ga, a positron emitter with 67 min half-life, the radiolabeling with gallium underwent a renaissance and also the clinical utility of ^{68}Ga citrate has been reevaluated.[19,20]

^{99m}Tc-citrate complex was described for the first time in 1967 and first biodistribution experiments of this radiotracer in mice were performed and compared with that of [^{99m}Tc]TcO_4^-.[21] Later on, ^{99m}Tc-citrate has been described as renal and tumor imaging agent[22,23,24] but it was Ercan et al. who introduced ^{99m}Tc-citrate as radiotracer for imaging inflammation in 1992 as a substitute for ^{67}Ga-citrate with the goal to overcome the drawbacks of the latter.[25] The authors induced bacterial abscesses in mice by injection of *Staphylococcus aureus* (*S. aureus*) and experimental arthritis in rabbits by application of ovalbumin und performed biodistribution studies and scintigraphy with both radiotracers. The maximum abscess/muscle ratios were found to be 4.0 for ^{99m}Tc-citrate at 1 h and 4.7 for ^{67}Ga-citrate at 4 h, comparable results were found in arthritic samples.

In a follow up study, ^{99m}Tc-citrate, ^{67}Ga-citrate, and **^{99m}Tc-methylene diphosphonate** (**^{99m}Tc-MDP**) were compared in rabbits with arthritic knees and in a limited number of patients with rheumatoid

arthritis.[26] The arthritic to normal knee ratios were 3.1 for ^{99m}Tc-citrate at 3h und 6.4 for ^{67}Ga-citrate at 6 h, respectively. Although the uptake of ^{99m}Tc-citrate was lower, the images were similar since ^{99m}Tc-citrate clearly showed synovial structures while ^{67}Ga-citrate remained in the surrounding inflammatory tissue. Biodistribution studies in mice and scintigraphic studies in humans indicated urinary excretion of ^{99m}Tc-citrate via kidneys, while with ^{67}Ga-citrate the liver and the biliary tract are the main excretory routes. ^{99m}Tc-citrate showed a high blood clearance resulting in a biological half-life of 36 min, while this value was for ^{67}Ga-citrate with 23 h much longer. In arthritic patients ^{99m}Tc-MDP and ^{99m}Tc-citrate showed both good accumulations at the inflamed site with increased bone uptake of ^{99m}Tc-MDP. In another osteoarthritic animal model with ^{99m}Tc-citrate the lesion-to-non-lesion ratio was found to be 4.1 and 3.1 after 30 min and 60 min, respectively.[27]

The ability of visualization of turpentine-induced inflammations with ^{99m}Tc-citrate was furthermore demonstrated in comparison with other ^{99m}Tc-complexes from gluconate, glucoheptonate, diethylene triamine pentaacetate, glucose phosphate, glucaric acid, malic acid and tartaric acid.[28,29] Compared with ^{99m}Tc-citrate, **^{99m}Tc-D-glucaric acid complex** showed likewise excellent properties for inflammation imaging. In another study, 18 patients with chronic osteomyelitis and 11 patients with benign bone disease underwent a ^{99m}Tc-citrate scan in comparison to ^{99m}Tc-MDP to evaluate both radiopharmaceuticals.[30] While ^{99m}Tc-MDP showed an uptake in all patients with bone disorders, ^{99m}Tc-citrate was able to identify those with osteomyelitis. In two studies it was confirmed that ^{99m}Tc-citrate has a better specificity in differentiating osteoblastic from degenerated bony lesions and that the ratio of ^{99m}Tc-citrate to ^{99m}Tc-MDP is a promising parameter to discriminate malignant from benign bone disease.[31,32]

That ^{99m}Tc-citrate may be useful for identification of acute pancreatitis was demonstrated at a cat animal model where an uptake ratio of 2.3 – 9.7 for pancreas to neighboring organs was found.[33]

Appendicitis is the most common abdominal inflammation and its clinical findings are clearly established. Nevertheless, the diagnosis may be unclear in infants and very young children. Therefore, radionuclide guided imaging of acute appendicitis would have a great diagnostic value. For that purpose a pilot study with ^{99m}Tc-citrate, ^{67}Ga-citrate, and **^{99m}Tc-dimercapto succinic acid** (**^{99m}Tc-DMSA**) was performed in rabbits with the result that ^{99m}Tc-citrate showed the best target-to-non-target ratio (2.67) and is preferable to the other radiotracers for visualization of appendicitis.[34] In a follow up study, 30 children with unclear diagnosis of appendicitis were evaluated; nineteen of them were confirmed with appendicitis by histological examination. ^{99m}Tc-citrate scan identified sixteen patients with acute appendicitis, one of them as false-positive and fourteen children without appendicitis, four of them false-negative.[35] In summary the authors recommended the use of ^{99m}Tc-citrate taking advantage of fast blood clearance, urinary excretion and low accumulation in other abdominal organs.

In an additional clinical study with patients suffering from active pulmonary tuberculosis ^{99m}Tc-citrate showed only a faint uptake in the lesion compared with ^{99m}Tc-DMSA[36] and in a further clinical example of a localized bowel loop inflammation the uptake of ^{99m}Tc-citrate was too transient in comparison with **^{99m}Tc-dextran**.[37]

Besides of abscess and inflammation, a potential tumor imaging with ^{99m}Tc-citrate was attempted on mice bearing transplanted EMT-6 tumors and Ehrlich ascites tumor models, whereby in both reports a certain tumor accumulation was observed.[23,38]

In the last decade the clinical application of the non-specific radiopharmaceutical ^{99m}Tc-citrate has significantly declined, as a detailed literature inquiry has resulted. The reason for that may be the growing distribution of the more easy available PET tracer [^{18}F]FDG providing similar information and yielding higher resolution images.

^{99m}Tc-antibiotics

Antibiotics, drugs that are inhibiting the growth and causing the death of bacteria, are commonly used for the treatment and prevention of bacterial infections and due to the strong interaction of the antibiotic with the infectious lesions the idea was, by making use of radiolabeled antibiotics, to achieve an *in vivo* imaging of infected areas. The first ^{99m}Tc-complex with an antibacterial compound was **^{99m}Tc-gentamicin** described in 1981 as radiotracer for renal studies.[39] Ercan et al. evaluated 1992 **^{99m}Tc-erythromycin** and **^{99m}Tc-streptomycin sulphate** for the visualization of inflammatory lesions in competition with ^{67}Ga-citrate.[40]

The most investigated antibiotic radiopharmaceutical was **^{99m}Tc-ciprofloxacin** (Infecton©) that has been introduced in 1997.[41] Ciprofloxacin is a 4-fluoroquinolone based broad spectrum antibiotic that is retained at infected sites and associates freely with metal ions, enabling the complex formation with technetium. The exact chemical structure of ^{99m}Tc-ciprofloxacin was for a long time unclear, until recently a Spanish group has synthesized an aqueous solution of ^{99}Tc-ciprofloxacin and analyzed it by ESI mass spectrometry. From the molar mass found, a ^{99}Tc/ciprofloxacin 1:2 ratio was reasonable and a cationic complex was suggested (Figure 2).[42]

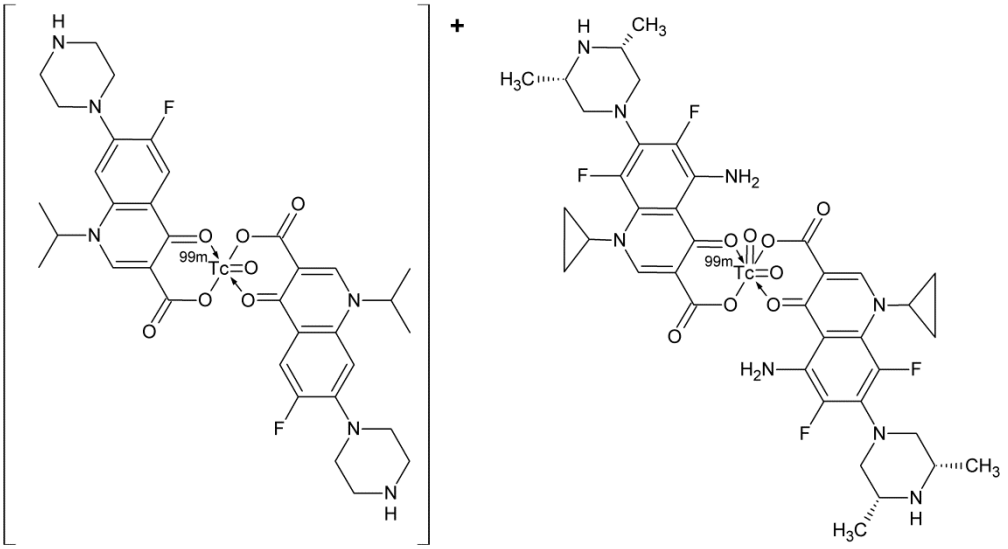

Figure 2. Suggested structure of **^{99m}Tc-ciprofloxacin**[42] (left) and **^{99m}Tc-sparfloxacin**[43] (right)

^{99m}Tc-ciprofloxacin has been comprehensively investigated for imaging of infectious diseases in humans, having a favorable biodistribution, low liver metabolism and a lack of bone marrow uptake as demonstrated in several clinical studies and summarized in profound review articles.[10,44,45] The largest study for ^{99m}Tc-ciprofloxacin was performed under supervision of the International Atomic Energy Agency (IAEA) with more than 900 patients with suspected bacterial infection.[46] This study resulted in an overall sensitivity of 85.4 % and a specificity of 81.7 % for detecting infectious lesions. Halder et al. synthesized two technetium-99m complexes; the **^{99m}Tc-oxo-ciprofloxacin** and the **^{99m}Tc(CO)$_3$-ciprofloxacin** and performed biodistribution and scintigraphic studies in rats with bacterial infection and sterile inflammation with comparable results.[47] Nevertheless there are still a number of controversial findings for imaging with ^{99m}Tc-ciprofloxacin, since it is proposed to bind to living bacteria only and not to dead and white cells, it should be capable to distinguish between bacterial infection and sterile inflammation, but this never has been confirmed. Some studies have revealed false positive uptake of ^{99m}Tc-ciprofloxacin also in sterile inflammation[44] and Palestro et al. found poor specificity and accuracy for ^{99m}Tc-ciprofloxacin in patients with osteomyelitis.[48] It was concluded, that the radiotracer will be inappropriate for imaging bacteria-specific infection.[10]

Another fluorinated quinolone, sparfloxacin having higher potency than ciprofloxacin, was radiolabeled with technetium-99m and evaluated regarding sterile and infectious inflammation in rabbits.[43] The proposed structure of **^{99m}Tc-sparfloxacin** is displayed at Figure 2. Scintigraphic imaging studies showed significant initial accumulation of the radiotracer in both turpentine oil-induced sterile inflammation as well as in *S. aureus* induced infection. However, rapid washout of tracer was noted from the sterile inflammatory lesions, while progressive concentration was observed in infected lesions, resulting in a fourfold increased tracer accumulation at the infected site at two hours post-injection.[43]

Further antibiotics carrying the fluoroquinolone pharmacophore have been used to form stable technetium-99m labeled complexes and in this regard studies with ^{99m}Tc-sparfloxacin,[49] -enrofloxacin[50], -lomefloxacin[51,52], -levofloxacin[53,51], -norfloxacin[54,51,55], -pefloxacin[56], -ofloxacin[51,57], -moxifloxacin[58], -prulifloxacin[59] and -gemifloxacin[60] have been performed. The corresponding ^{99m}Tc-complexes were synthesized not only starting from [^{99m}Tc]pertechnetate, but also by using a *fac*-[^{99m}Tc(CO)$_3$(H$_2$O)$_3$]$^+$ precursor[51,57] or a [^{99m}TcNL$_x$] core[54], the suggested structures for **^{99m}Tc-ofloxacin** and **^{99m}Tc-norfloxacin dithiocarbamate** are displayed at Figure 3, respectively. Biodistribution results in bacterial infected mice showed that ^{99m}Tc-norfloxacin had a higher uptake at the infected sites and a better abscess/muscle ratio than those of ^{99m}Tc-ciprofloxacin.[54] In a study using four technetium-99m labeled fluoroquinolones, the biodistribution results in rats showed substantial accumulation at the focal infection site but also a high accumulation in liver and kidneys.[51] These findings were confirmed by SPECT imaging of rats with bacterially induced intramuscular infection.

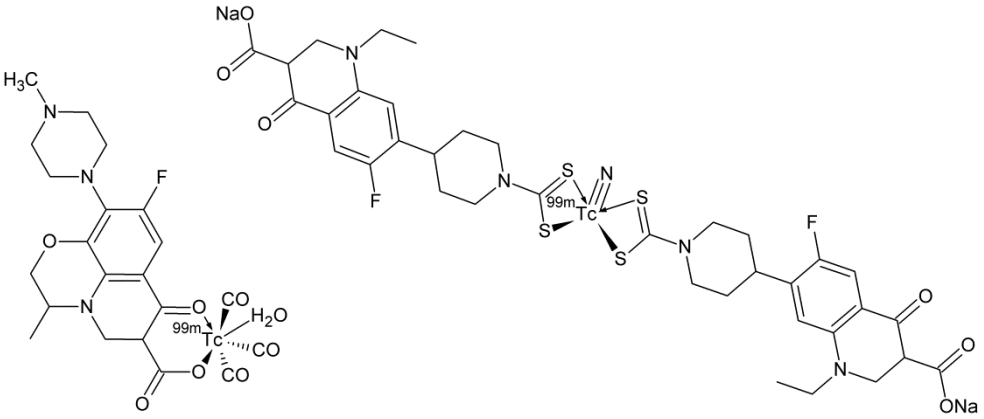

Figure 3. Proposed structure of **^{99m}Tc(CO)$_3$-ofloxacin**[57] (left) and **^{99m}Tc-norfloxacin dithiocarbamate** complex (right)[54]

Ceftizoxime is a broad-spectrum antibiotic from the class of cephalosporins interacting to the bacterial cell wall and causing wall ruptures with the result of killing the bacteria. A **^{99m}Tc-ceftizoxime** kit preparation was described in 2005 and biodistribution experiments and SPECT investigations in rats with bacterial muscle infection (*Escherichia coli* (*E. coli*)) were performed indicating a clear uptake of the radiotracer.[61] To differentiate inflammatory and infectious processes ^{99m}Tc-ceftizoxime was injected in rats with both lesions and scintigraphic imaging was performed. Quantitative analysis showed a target-to-non-target ratio of 2.37 after 2 h for the infected area in comparison with 1.5 for the inflammation. Hence, the authors postulated that ^{99m}Tc-ceftizoxime is able to distinguish aseptic from septic inflammatory processes.[62] For imaging of osteomyelitis ^{99m}Tc-ceftizoxime was loaded on long-circulating pH-sensitive liposomes and SPECT images of bone infected rats were recorded with the result, that at 8 h in osteomyelitis-bearing animals a target-to-non-target ratio of 2.25 could be

observed.[63] In a recent study on the efficacy of ^{99m}Tc-ceftizoxime in the diagnosis of subclinical infections associated with implants, rats which received bacterial contaminated titanium implants were injected with the radiotracer three weeks after surgery.[64] According to the scintigraphic images ^{99m}Tc-ceftizoxime showed affinity to the periprosthetically infected areas. Furthermore, it was demonstrated in animal experiments that ^{99m}Tc-ceftioxime may be used for detection of wound infection after sternotomy.[65]

Further antibiotics from the class of cephalosporins like cefoperazone, ceftriaxone and cefuroxime have been radiolabeled with ^{99m}Tc and evaluated in bacterial infected animals. So for **^{99m}Tc-cefoperazone**[66] at the site of infection a target-to-non-target ratio of 4.5 was found, the corresponding values for **^{99m}Tc-ceftriaxone**[67] and **^{99m}Tc-cefuroxime**[68] were 5.6 and 1.8, respectively. The preparation, stability, and evaluation of **^{99m}Tc-cefuroxime axetil**, an orally available ester prodrug of the antibiotic, was successfully performed, with the result that the radiotracer showed a higher retention in septic inflamed than in sterile inflamed areas.[69,70] For differentiation of bacterial infection and sterile inflammation, animal models induced with *S. aureus*, *E. coli* and turpentine oil-induced inflammation were evaluated with ^{99m}Tc-ceftriaxone giving after 4 h lesion-to-normal ratios of 2.36, 12.66, and 1.40, respectively.[71] The high radiotracer accumulation in *E. coli* infected areas indicates an increased affinity of ^{99m}Tc-ceftriaxone to gram-negative bacteria and the significant difference between infection and inflammation let the authors conclude that this radiotracer might be specific for bacterial infection but not for sterile inflammation. A similar study was performed with ^{99m}Tc-ceftriaxone where in animal models with turpentine oil-induced sterile inflammation at 4 h a target-to-non-target ratio of 1.5 was observed, while with *S. aureus* infected animals a ratio of 3.6 was observed.[72] These findings were confirmed when ^{99m}Tc-ceftriaxone was used in patients with bacteria-induced osteomyelitis showing a progressive increase in radiotracer uptake as demonstrated by SPECT/CT fusion images.[72] The authors also proposed a structure of the ceftriaxone technetium-99m complex, which is displayed at Figure 4.

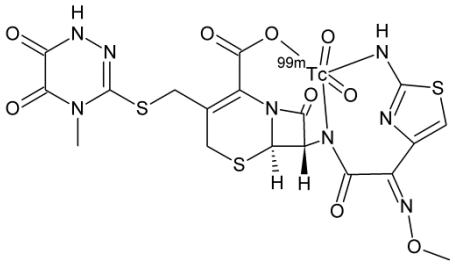

Figure 4. Proposed structure of **^{99m}Tc-ceftriaxone**[72]

To detect tuberculosis induced infections, specific anti-tuberculous drugs like ethambutol and isoniazid have been likewise radiolabeled with technetium-99m.[44] **^{99m}Tc-ethambutol** was produced via the direct labeling method and a clinical trial with 14 patients demonstrated the specificity and sensitivity of the radiotracer for detection of pulmonary and bone tubercular lesions and its safe use for human application.[73] **^{99m}Tc-alignate-isoniazid** loaded microspheres were prepared for determination of biodistribution in mice and revealed a significant accumulation in the lungs.[74]

Vancomycin is a glycopeptide antibiotic with a molar weight of 1450 Dalton and is applied in cases of bacteria cultures showing extremely high resistance. Biodistribution studies of **^{99m}Tc-vancomycin** resulted in a significant higher accumulation at *S. aureus* infected rats whereas the uptake in animals with turpentine-induced inflammation was quite low.[75] An interesting pretargeting strategy was suggested by Vito et al. who formed a *trans*-cyclooctene-vancomycine derivative which was coupled with a ^{99m}Tc-hynic-tetrazine complex and showed a 2.5– to 3-fold uptake in a *S. aureus* infected mice model.[76] In recent time, further antibiotics like clindamycin[77], doxycycline[78], amoxicillin[79] and cefepime[80] have been evaluated for bacterial infection imaging, whereby for **^{99m}Tc-cefepime** a bacterial infected-to-non-infected-tissue ratio of about 8.4 was found, which is significantly higher than for ^{99m}Tc-ciprofloxacin, qualifying ^{99m}Tc-cefepime as suitable radiotracer for infection imaging.[80]

Alafosfalin or (S)-alanyl-(*R*)-1-aminoethylphosphonic acid is broad-spectrum antibacterial peptide and was likewise radiolabeled with technetium-99m in a kit formulation. Comparison experiments with ^{67}Ga-citrate[81] at one hand and ^{99m}Tc-DTPA and ^{99m}Tc-labeled leucocytes on the other hand revealed that **^{99m}Tc-alafosfalin** accumulated better at infected sites than ^{99m}Tc-DTPA but less than the ^{99m}Tc-labeled leucocytes.[82]

Vitamin B_{12} (cobalamin, Cbl) is an important enzyme cofactor required in fast replicating cells like bacteria and its distinct uptake mechanism may represent the background for radiolabeled derivatives for targeting bacterial infections. For that reason the vitamin B_{12} anion, modified with a NHO donor set was radiolabeled with the $[^{99m}Tc(OH_2)_3(CO)_3]^+$ complex to form **^{99m}Tc-PAMA(4)-Cbl**, with the proposed structure displayed at Figure 5.[83] This radiotracer was evaluated for specific targeting *E. coli* and *S. aureus in vitro* and in a cage model of foreign body infection in mice. The subcutaneously implanted cage model allowed the induction of a local persistent infection with a high and reproducible bacterial density. In summary, ^{99m}Tc-PAMA(4)-Cbl showed a significant higher retention in bacterially infected cages than in non-infected animals.

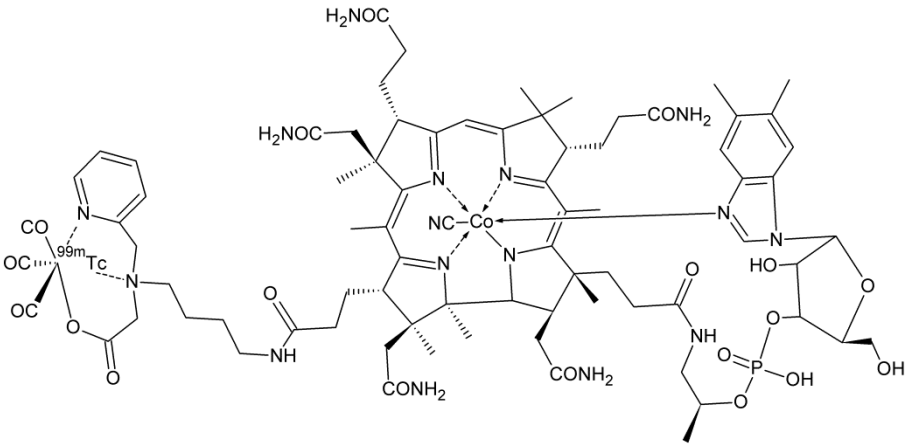

Figure 5. Structure of **^{99m}Tc-PAMA(4)-Cbl**[83]

^{99m}Tc-antifungal agents

The concept of handling radiolabeled antibiotics has been further extended to antifungal agents since fungal infections are life-threatening, especially in surgical patients. Thus, the detection and elimination of the primary focus of fungal infection and the discrimination from sterile inflammation would be extremely useful for selection and length of the corresponding therapeutic methods. *Candida albicans* (*C. albicans*) and A*spergillus fumigatus* (*A. fumigatus*) are known to be the mostly appearing fungi and the major cause for systemic infections, accordingly antifungal agents as e.g. fluconazole were radiolabeled with technetium-99m. Lupetti et al. described the first **^{99m}Tc-fluconazole** complex by direct radiolabeling of fluconazole with [^{99m}Tc]pertechnetate and evaluated it in mice, infected with C*. albicans* and S*. aureus*.[84] Even though fluconazole is a simple molecule containing two triazole and one difluorophenyl moieties, any information about the structure of the formed technetium-99m complex is not provided in the literature so far. ^{99m}Tc-fluconazole detected *C. albicans* but not *A. fumigatus* caused infections without visualizing bacterial infections and sterile inflammation, so it was concluded to be a selective tracer for *C. albicans*.[84] In a follow-up study, Lupetti et al. compared the efficacy of ^{99m}Tc-fluconazole for *C. albicans* induced infections with that of ^{99m}Tc-labeled antifungal peptides and came to the conclusion that neither ^{99m}Tc-fluconazole nor the ^{99m}Tc-peptides are optimal radiotracers for imaging fungal infections.[85] They proposed that other radiolabeled antifungal agents like **^{99m}Tc-voriconazole** and **^{99m}Tc-caspofungin** are more promising.

Encapsulation of pharmaceuticals in nanoparticulate carriers is commonly used with the objective of modifying the pharmacokinetic of drugs, resulting in a more efficient treatment. For modification of the *in vivo* release profile of ^{99m}Tc-fluconazole**,** the radiotracer was encapsulated in conventional and surface-modified nanocapsules with a diameter of 236-356 nm.[86] The surface-modified (PEGylated) nanocapsules offered advantageous properties as delivery system of ^{99m}Tc-fluconazole by showing a

reduced drug release as a result of minor interaction with plasma proteins. But whether these radiotracer containing nanocapsules would result in a long-circulating intravenous formulation of ^{99m}Tc-fluconazole has still to be demonstrated by *in vitro* studies.

Caspofungin is a lipopeptide of fungal origin that irreversibly inhibits an enzyme which is essential for the synthesis of 1,3-ß-D-glucan, a key compound of the fungal cell wall and essential for osmotic stability. The amino- and hydroxyl moieties of caspofungin can interact with the *fac* $[^{99m}Tc(CO)_3(H_2O)_3]^+$ precursor to form a **^{99m}Tc-(CO)$_3$-caspofungin** complex whose proposed chemical structure is displayed at Figure 6.[87] Biodistribution of ^{99m}Tc-(CO)$_3$-caspofungin in normal mice showed high hepatic uptake (22 %) in combination with low renal elimination and slow blood clearance, indicating high binding to plasma proteins. After 3 hours the uptake in sterile inflammation and *C. albicans* induced injury was 4.7 and 5.7 % ID/organ, respectively. However, no significant uptake of the radiotracer could be observed in *Aspergillus niger* (*A. niger*) induced infection.

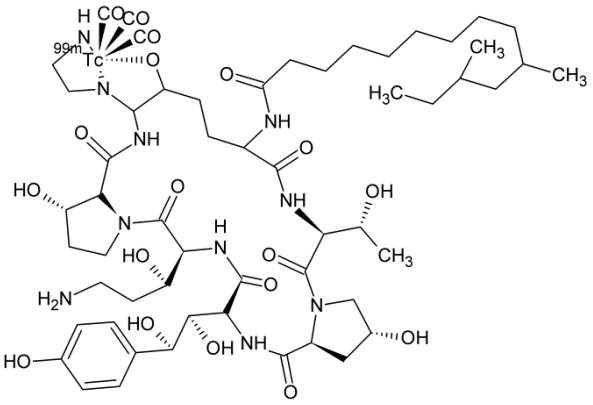

Figure 6. Proposed structure of **^{99m}Tc-(CO)$_3$-caspofungin**[87]

Because chitin is an important constituent of many fungal cell walls, but does not occur in bacterial cells, this carbohydrate polymer might represent a selective target for development of radioligands to detect fungal infections. Therefore a chitin binding protein produced by *Serratia marcescens* named CBP21 has been radiolabeled with technetium-99m to form a radiotracer, specific for fungal infections. The radiolabeling with ^{99m}Tc was performed via the bifunctional chelating group succinimidyl hydrazinonicotine amide (s-HYNIC) and the **^{99m}Tc-HYNIC-CBP21** was used for performing *in vitro* binding studies with polymorphic chitin forms and *in vivo* investigations in mice with bacterial and fungal infections.[88] *In vivo* best rates of fungal infection versus bacterial infection were observed at 5 and 7 h (3.6 and 2.9 % ID/g, respectively) post injection of the tracer, maximum uptake detected in *A. fumigatus* induced infections in mice was 0.63 %ID/g.

A challenging method for targeting fungal infections was chosen by the Hnatowich group. They used radiolabeled morpholino oligomers (MORFs), DNA analogs in which the sugar is replaced by a

morpholino moiety, for targeting the ribosomal RNA of fungi.[89] Two ^{99m}Tc-labeled fungal MORF probes, a genus specific probe against *Aspergillus* (AGEN) and a species specific probe against *A. fumigatus* (AFUM) were designed and conjugated with technetium-99m via NHS-mercaptoacetyl triglycine (NHS-MAG_3). The biodistribution of **^{99m}Tc-AGEN** and **^{99m}Tc-AFUM** and SPECT/CT imaging was performed in mice with *A. fumigatus* infection in the lungs. The animals with pulmonary infections administered with ^{99m}Tc-AGEN and ^{99m}Tc-AFUM showed immediate and obvious accumulation in the infected lungs and reached 2.0 and 2.7 fold higher uptake than the controls.

^{99m}Tc-antimicrobial peptides

Antimicrobial peptides are important components of the innate immune system of all living organisms, often containing hydrophobic and cationic amino acids, which are organized in an amphipathic structure.[90] Most antimicrobial peptides interact by their cationic domains with the negatively charged surface of the microorganisms. The challenge of purifying natural antimicrobial peptides has prompted their recombinant production by genetically engineered bacteria or via peptide synthesis.[90] On the basis of the chemical characteristics, i.e. amino acid sequence present in natural antimicrobial peptides, special sequences interacting with the microorganisms, such as human lactoferrin (hLF), ubiquicidin (UBI) and other members of the defensin family have been identified as promising candidates for radiolabeling. These peptides demonstrated chemo-attractive activity for monocytes and lymphocytes and, exemplarily, the accumulation of **^{99m}Tc-labeled human neutrophil peptide-1** in bacterial infected mice was reported.[91] An overview about radiolabeled antimicrobial peptides as infection imaging agents as well as about the key features of antimicrobial peptides is given in some excellent review articles. [10,44,90,92,93]

Among the human-derived antimicrobial peptides tested, the UBI 29-41, a small synthetic peptide (1,693 Da) binding *in vitro* preferentially to bacteria and not to leukocytes, showed the greatest promise. (Figure 7) UBI 29-41 has displayed specificity for *C. albicans* and *A. fumigatus* caused infections and is also able to distinguish *S. aureus* infections from *E. coli* induced infections.[94]

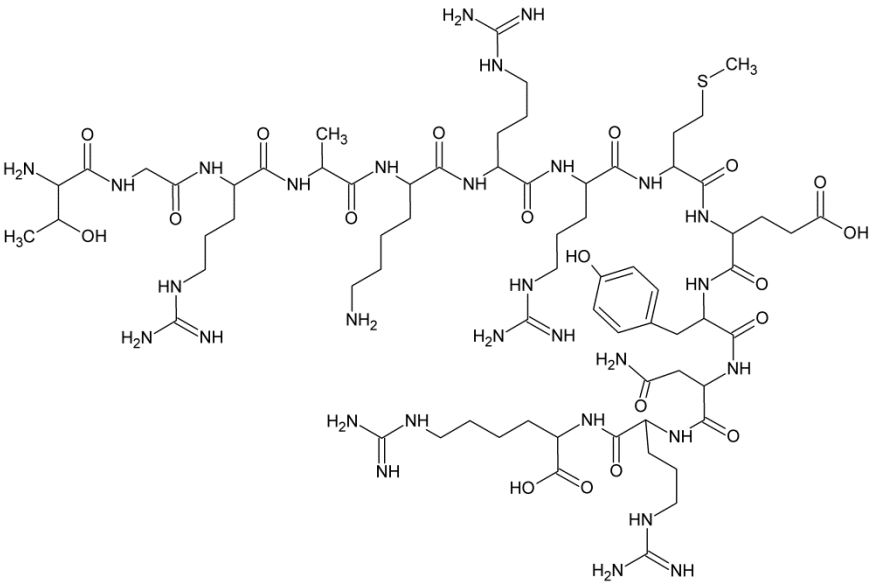

Figure 7. Structure of UBI 29-41[44]

First radiolabeling of UBI 29-41 with technetium-99m was performed by Welling et al. by making use of the direct method; although the structure of the **^{99m}Tc-UBI 29-41** complex is difficult to predict, a single radiolabeled product with more than 95 % purity was formed.[95] *In vivo* scintigraphy demonstrated accumulation of ^{99m}Tc-UBI 29-41 in *S. aureus* infected mice, which could be decreased by prior injection of unlabeled UBI 29-41. In case of ^{99m}Tc-UBI 29-41 and considering that five of the thirteen amino acids of UBI are arginine, it was questionable if some of these groups could form a stable complex with reduced technetium; therefore the specific coordination of the ^{99m}Tc-UBI 29-41 complex was determined through quantum-mechanical calculations.[96]

Furthermore a **^{99m}Tc-HYNIC-UBI/tricin** based complex was synthesized and compared regarding *in vitro* stability with the direct labeled ^{99m}Tc-UBI 29-41. The *in silico* calculations suggested that the Arg^7 and Lys amino group are highly specific coordination sites for the Tc(V)O cation, additionally stabilized by two H_2O molecules. To find well defined complex structures between technetium-99m and UBI 29-41 the peptide was radiolabeled using a PEGylated *N*-(*N*-(3-diphenylphosphinopropionyl)glycyl)-*S*-tritylcysteine ligand (PEG-PN_2S).[97] The so formed **^{99m}Tc-PN_2S-PEG-UBI** was compared with ^{99m}Tc-UBI 29-41 in mice infected with *S. aureus*. As result both technetium-99m complexes proved to be equally effective in detecting infected sites; however, the ^{99m}Tc-PN_2S-PEG-UBI showed *in vivo* higher protein binding values, followed by a lower renal clearance.

To evaluate if ^{99m}Tc-UBI 29-41 is bound to the bacterial cell envelope simply by nonspecific electrostatic interaction, a comparative study of the *in vitro* binding of ^{99m}Tc-UBI 29-41 and two different ^{99m}Tc-labeled cationic peptides was conducted.[98] While the binding of the other labeled cationic peptides to tumor cells was 33-41 %, the binding of ^{99m}Tc-UBI 29-41 was much lower being

less than 4 %. *In vivo* studies revealed a significant difference in the radioactivity accumulation of ^{99m}Tc-UBI 29-41 between the sites of infection and inflammation (2.08 fold) compared to ^{67}Ga-citrate (1.14 fold).[98]

The feasibility that ^{99m}Tc-UBI 29-41 could be used for monitoring the efficacy of antibacterial agents was investigated by scintigraphy of *S. aureus* infected animals with the radiotracer after treatment with Cloxacillin or Erythromycin.[99] Decreasing amounts of ^{99m}Tc-UBI 29-41 uptake correlated with increasing doses of the antibiotic agents and corroborated the theory. In a similar manner the uptake of ^{99m}Tc-UBI 29-41 was evaluated at bacterial infected sites in rabbits before and after treatment with ciprofloxacin.[100] Also in that case the scintigraphic images showed after ciprofloxacin treatment a decreased target-to-non-target ratio on day 3 and day 5 what was in correlation with the number of viable bacteria.

In another study ^{99m}Tc-UBI 29-41 was evaluated as bacterial infection-seeking agent in *S. aureus* and *E. coli* infected rabbits, additionally turpentine oil-induced sterile muscle inflammation was evaluated with the radiotracer.[94] In summary, a significant higher accumulation was observed at the *S. aureus*-infected animals compared with the *E. coli*-infected sites, while in sterile inflamed tissue no tracer uptake was noticed.

First clinical trials with ^{99m}Tc-UBI 29-41 were published in 2004 [101], six children with suspected bone infection; and 2005, eighteen patients with suspected bone, soft-tissue, or prosthesis infections.[102] Pharmacokinetic evaluation demonstrated fast blood clearance with mean residence time of 0.52 h; approximately 85 % of the injected activity was eliminated by renal clearance 24 h after ^{99m}Tc-UBI 29-41 administration; images showed an average target-to-non-target ratio of 2.18 in positive lesions at 2h.[101] In the 18 patients involving study, 14 cases showed positive findings with a maximum target-to-non-target ratio of 2.75 at 30 min which decreased to 2.04 at 120 min.[102] In a subsequent clinical trial, thirteen patients with suspected mediastinitis after cardiac surgery were subjected to ^{99m}Tc-UBI 29-41 scintigraphy.[103] Qualitative analysis correctly identified 5/6 patients with mediastinitis, in addition with six true-negative results.

For discrimination between infected and uninfected prosthetic joints in a rabbit model, left knee arthroplasty was performed and the joint was infected by injection of either *S. aureus* or sterile saline for negative control. Scintigraphy with ^{99m}Tc-UBI 29-41 was performed on day 9 and 20 after surgery and the operated-to-normal knee activity ratio was calculated.[104] A slightly higher accumulation was observed in the infected animals while in chronic sterile periprosthetic inflammation all scans were truly negative.

A **^{99m}Tc-tricin-HYNIC-UBI 29-41 complex** was synthesized by using freeze-dried kit formulations and applied to patients with suspected bone or soft-tissue infections.[105] The biodistribution of the radiotracer showed rapid accumulation of activity in the kidneys in the first 30 min after injection,

which gradually declined and accumulated in the urinary bladder. Scintigraphy showed minimal accumulation in non-target tissues with an average target-to-non-target ratio of 2.1 in positive lesions at 30 min.

In the past, further clinical studies with ^{99m}Tc-UBI 29-41 as infection seeking agent have been published; i.e. the detection of suspected bacterial infection at diabetic foot patients[106], patients with suspected osteomyelitis in comparison with **^{99m}Tc-MDP**[107], cases with orthopedic implant infection[108,109] and patients having other musculoskeletal infections.[110] As consequence for the increasing need and to have standardized synthesis conditions a two component kit system for easy preparation of ^{99m}Tc-UBI 29-41 was recently presented.[111]

Besides of all the positive clinical results obtained with ^{99m}Tc-UBI 29-41 there is also one study where the distribution of the SPECT tracer was compared with its ^{18}F-labeled analog (**^{18}F-UBI 29-41**) in *S. aureus*-infected rats without observing a specific binding.[112] Interestingly, two different ^{18}F-labeled UBI derivatives, **^{18}F-UBI 28-41** and **^{18}F-UBI 29-41**, both labeled via the [^{18}F]SFB (*N*-succinimidyl-4-[^{18}F]fluorobenzoate) method, were included in the study. All radiolabeled UBI derivatives exhibited variably increased uptake in the bacterial infected areas, but in no case a clear congruity of tracer accumulation with the distribution of *S. aureus* was established. As possible explanation the authors postulated that the bacteria may be encapsulated in the center of the abscess and consequently the UBI derivatives could not bind; but this raises the question for the general mechanism of the *in vivo* binding of radiotracers to bacteria.

^{99m}Tc-cyclooxygenase-2 inhibitors

The enzyme cyclooxygenase-2 (COX-2) is an inducible isoform of the cyclooxygenase family and is expressed in contrast to the COX-1 as a result of an inflammatory stimulation. The functional expression of COX-2 leads to high levels of eicosanoids which subsequently are mediating pain and fever and trigger acute and chronic inflammatory processes. For inhibition of COX-2, anti-inflammatory drugs like aspirin or ibuprofen are traditionally applied; furthermore COX-2 selective inhibitors like celecoxib or parecoxib were used to suppress acute inflammation and pain. The monitoring of inflamed areas and the detection of chronically inflamed tissue may be achieved by visualization of the COX-2 with radiolabeled COX-2 inhibitors; what is a considerable challenge in radiopharmaceutical probe development. For that purpose a huge number of radiotracers labeled with fluorine-18 and carbon-11 has been designed and evaluated, to obtain suitable PET tracers, but until now no compound has achieved a clinical application yet.[113,114] Surprisingly, albeit technetium-99m has had a main impact on radiotracer development, only a handful of ^{99m}Tc-labeled COX-2 inhibitors have been described so far.

Diflunisal (5-(2',4'-difluorophenyl)salicylic acid) inhibits non-selectively COX-1 and COX-2 and was radiolabeled in 2002 by addition of stannous tartrate to a mixture of [^{99m}Tc]TcO_4^- and a diflunisal solution. The formed **^{99m}Tc-diflunisal complex** was applied as ophthalmic solution for detection of the external lacrimal drainage system in the eye, since the COX enzyme is also located in this area, and was the first example of a ^{99m}Tc-labeled COX-2 inhibitor.[115]

Celecoxib (4-[5-(4-(methyl)phenyl)-3-(trifluoromethyl)-1*H*-pyrazol-1-yl]benzenesulfonamide), a selective COX-2 inhibitor, has been approved for clinical use in treatment of osteoarthritis or rheumatoid arthritis; hence, efforts were undertaken to radiolabel celecoxib with technetium-99m. Because inhibition of COX-2 also causes delayed tumor growth in xenograft models, e.g. one study aimed to assess the clinical endpoints of celecoxib treatment by visualization of the COX-2 expression with ^{99m}Tc-labeled celecoxib.[116] *L,L*-ethylene dicysteine (EC) which is known to form stabile N_2S_2 chelates with technetium-99m, was coupled to the sulfonamide moiety of celecoxib and the resulting EC-celecoxib ligand (Figure 8) was used for direct radiolabeling with [^{99m}Tc]TcO_4^- in presence of $SnCl_2$, Na_2HPO_4, ascorbic acid and glutamic acid to form the **^{99m}Tc-EC-celecoxib** complex.

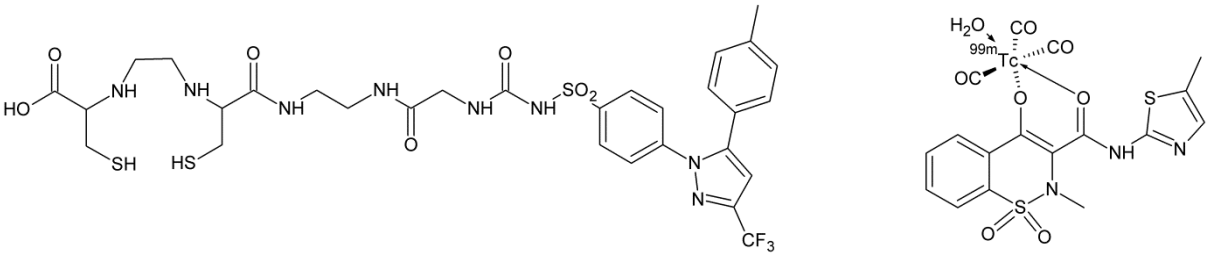

Figure 8. Structure of the ***L,L*-ethylenedicysteine-celecoxib** ligand[116] (left) and proposed structure of the **^{99m}Tc-$(CO)_3$-meloxicam** complex[117] (right)

Biodistribution studies of ^{99m}Tc-EC-celecoxib in breast tumor bearing rats and planar scintigraphy was performed in mice, rats, and rabbits. The *in vivo* tissue distribution of the radiotracer showed increased tumor-to-tissue ratios as a function of time (tumor-to-muscle ratio of 4.3 at 30 min and 9.7 at 4h). Planar images confirmed that the tumors could be visualized from 0.5 to 4 h in the animal models and after estimation of the dosimetry absorption of patients the authors concluded that **^{99m}Tc-EC-celecoxib** might be useful for clinical evaluation after treatment with COX-2 inhibitors.

For monitoring induced arthritis in rats celecoxib was directly labeled with technetium-99m; in parallel ^{99m}Tc-loaded albumin microspheres (CMs) were incubated with celecoxib, to form a **^{99m}Tc-CMS-celecoxib** complex.[118] *In vitro* release studies indicated that the microspheres sustained the release of the drug for approximately 6 days. Organ distribution showed a significant amount of ^{99m}Tc-celecoxib in liver and spleen while in case of ^{99m}Tc-CMS-celecoxib a significant amount of

radioactivity accumulated in the lungs. By observing the tracer accumulation in the inflamed and non-inflamed joints ^{99m}Tc-celecoxib showed no significant differences, while ^{99m}Tc-CMS-celecoxib displayed a 2.5-fold higher uptake. This finding may be a result of the prolonged circulation of ^{99m}Tc-CMS-celecoxib in the blood.

A further example of direct labeled **^{99m}Tc-celecoxib** was presented at 2011, where the labeling conditions have been optimized to be performed at 25°C, pH=7 with 500 µg of celecoxib and 500 µg of stannous chloride.[119] Biodistribution data of ^{99m}Tc-celecoxib in mice with sterile turpentine oil-induced inflammation revealed a slightly higher uptake in the inflamed areas as displayed in target-to-non-target ratios of 1.6, 2.0, and 2.4 at 15 min, 1 h, and 4h post injection of the radiotracer, respectively.

That ^{99m}Tc-celecoxib indicates selectivity towards cancerous tissue can be reasoned from a preliminary study including rats with 1,2-dimethylhydrazine induced colon cancer. Scintigraphic images at 4 h post injection of ^{99m}Tc-celecoxib showed significant uptake of the radiotracer in the tumor site with proven histopathological changes.[120]

Meloxicam was developed as non-steroidal anti-inflammatory drug and is clinically approved for treatment of arthritis and inflammatory lesions. It is an unselective COX-inhibitor, slightly more sensitive for COX-2 (IC_{50}=4.7µM) than for COX-1 (IC_{50}=36µM).[121] Meloxicam was directly labeled with technetium-99m by addition of [^{99m}Tc]TcO_4^- solution to an isotonic mixture of the COX-inhibitor and stannous chloride.[122] The obtained **^{99m}Tc-meloxicam** complex was found to be stable for up to 24h at room temperature; and its biodistribution in with *E. coli* inflamed mice was studied. The radioactivity uptake ratios between normal and inflamed muscles detected at 2, 4, and 24 h post injection of ^{99m}Tc-meloxicam were 3.1, 5.1, and 8.4, respectively, indicating that this radiotracer is able to localize inflamed lesions and may be useful as an inflammatory imaging agent. In another study with meloxicam, the radiolabeling was performed by using the $[^{99m}Tc(CO)_3(H_2O)_3]^+$ precursor to form a **^{99m}Tc-$(CO)_3$-meloxicam complex**, its proposed structure is displayed at Figure 8.[117] Radiochemical stability of the ^{99m}Tc-$(CO)_3$-meloxicam in human serum was >86 % up to 24 h and additional studies showed that 72 % was transferred to serum proteins indicating a high protein binding. The partition coefficient (log*P*) of the radiotracer in octanol/water was found to be 0.098, what is remarkably low. The radioactivity uptake ratios of ^{99m}Tc-$(CO)_3$-meloxicam by turpentine oil-induced inflamed muscle to normal muscle were 3.08, 3.90, and 4.62 at 1 h, 4 h, and 24 h post injection, respectively. The increase of the target-to-non-target ratio by the time may be a result of the clearance of nonspecific uptake of the radiotracer from normal tissue. By comparing the ^{99m}Tc-meloxicam with the ^{99m}Tc-$(CO)_3$-meloxicam it was concluded that the binding of the radiotracers at the inflamed site was comparable, however, the biodistribution pattern was favorable for the radiotracer carrying the tricarbonyl core due to decreased background activity especially in the abdominal region.

Piroxicam, another COX-inhibitor possessing a similar structure as meloxicam, was likewise directly labeled with technetium-99m and the obtained **^{99m}Tc-piroxicam** showed good accumulation in bacterial (*E. coli*) inflamed tissue and turpentine oil-induced sterile inflammation.[123] The target-to-non-target uptake ratios for both septic and sterile inflamed mice were 8.7 and 10.6 at 24 h post injection, respectively.

In order to optimize the therapeutic efficacy of existing nonsteroidal anti-inflammatory drugs (NSAIDs) like indomethacin, ketoprofen, ibuprofen, naproxen, and others, the corresponding tropinol esters of these compounds were synthesized. As the anti-inflammatory activity of these new compounds was equal or higher than that the parent drugs and simultaneously their resistance toward enzymatic hydrolysis was increased, Yadav *et al.* performed the radiolabeling of these NSAID-tropinol esters with technetium-99m.[124] This was realized by direct reaction of the NSAID-tropinol ester with [^{99m}Tc]TcO_4^- in presence of stannous chloride and acetic acid and the labeling efficiency was found to be 84-97 % depending on time, pH, and solvent. Sprague-Dawley rats carrying carrageenan-induced inflammation and induced arthritis in the hind paws were subjected to scintigraphy with the **^{99m}Tc-tropinol-NSAIDs** and exhibited selective accumulation of the radiotracers at the inflamed sites.

Diclofenac, another NSAID with high affinity to COX-1 (IC_{50}=60 nM) and moderate affinity to COX-2 (IC_{50}=200 nM), is clinically approved for treatment of rheumatoid arthritis and osteoarthritis. The **^{99m}Tc-diclofenac** obtained by the reaction of [^{99m}Tc]pertechnetate and stannous chloride was evaluated in mice bearing a bacterial induced (*E. coli*) infection or sterile inflamed (turpentine oil) inflammation model.[125] The uptake ratios in the inflamed and contralateral tights were evaluated. In case of bacterial infection the target-to-non-target ratio only slightly exceeded unity, whereas in the case of sterile inflammation it reached 4.46 at 2 h post injection. Therefor the authors concluded that ^{99m}Tc-diclofenac allows differentiation between sterile and non-sterile inflammation.

To underline the importance of the topic, recently a patent study was published, describing a variety ^{99m}Tc-labeled non-steroidal anti-inflammatory drugs, such as rofecoxib, indomethacin, naproxen, and ketorolac with the aim of identifying inflamed and tumor tissue, characterized by increased COX expression.[126]

Summary and Conclusions

Recent improvements in multimodal imaging have provided the modern clinician with an appropriate tool box for, on the one hand, sensitive and accurate localization of inflammatory or infected lesions and, on the other hand, functional characterization of the underlying disorder. In particular, nuclear medicine techniques increasingly play an important role by providing objective biomarkers for

personalized medicine. Technetium-99m-labeled radiotracers and SPECT made a decisive contribution to this. These techniques offer the widespread possibility to specifically target cells and molecules that are involved for cell and tissue characterization, differential diagnosis, selection of patients for targeted therapies, prediction and follow-up of therapy response.

A number of ^{99m}Tc-labeled, inflammation seeking radiopharmaceuticals has been employed and applied with promise in clinical settings. ^{99m}Tc-citrate was successfully used in patients with arthritis[26], chronic osteomyelitis and benign bone disease[30] and in children with unclear diagnosis of appendicitis.[35] Radiolabeled antibiotics like ^{99m}Tc-ciprofoxacin, underwent a wide clinical scope, studying more than 900 patients with suspected bacterial infection[46]; another antibiotic, ^{99m}Tc-ceftriaxone demonstrated success in patients with bacteria-induced osteomyelitis.[72] ^{99m}Tc-ethambutol was effectively used for the detection of pulmonary and bone tubercular lesions.[73] Furthermore, the ^{99m}Tc-labeled antimicrobial peptide UBI 29-41 was applied multiple times: in children with suspected bone infection[101], patients with soft-tissue or prosthesis infections[102,108,109], cases of suspected mediastinitis after cardiac surgery[103], or suspected osteomyelitis.[107]

Aside from these successful applications, also some controversial results with radiotracers for inflammation have been discussed[44,48,112], indicating that the research in this field must be encouraged and accelerated in order to meet the above mentioned clinical challenges. The providing of convenient and safe-to-handle labeling kits is one precondition for the broader use of ^{99m}Tc-labeled inflammation seeking radiotracers[61,82,105,111]; up to now there is none of these radiopharmaceuticals commercial available. Additionally the physical properties of recently available radionuclides, e.g. ^{68}Ga should be considered to reevaluate former developed radiopharmaceuticals like ^{99m}Tc-citrate.[19,20]

An ongoing subject in nuclear medicine is the imaging and therapy of malignant neoplastic diseases. In this regard, the correlation between inflammation and cancer is widely accepted and e.g. ^{99m}Tc-citrate was attempted for tumor imaging[23,38]. COX-2 overexpression was shown to be also implicated in inflammogenesis of cancer[127,128] and radiotracers like ^{99m}Tc-labeled celecoxib proved to be promising as tumor imaging agent.[116] In this regard the future development of COX-2 inhibitors radiolabeled with short-lived radioisotopes (^{18}F, ^{68}Ga) and radiometals with longer half-live like ^{99m}Tc, ^{64}Cu, and ^{44}Sc hold promise as successful radiopharmaceuticals targeting inflammation and infection and inflammatory induced cancerous diseases. Further efforts in this field are needed to transfer potential candidates into clinical practice.

Acknowledgements

The authors thank the Helmholtz Association for funding a part of this work through Helmholtz-Portfolio Topic “Technologie und Medizin − Multimodale Bildgebung zur Aufklärung des In vivo-Verhaltens von polymeren Biomaterialien”. This work also is part of the research initiative “Radiation-Induced Vascular Dysfunction (RIVAD)”.

Conflict of interest

The authors declare that they have no conflict of interest.

References

1. S. J. Goldsmith and S. Vallabhajosula, *Semin Nucl Med*, 2009, **39**, 2-10.
2. C. Girlich, D. Schacherer, P. Lamby, M. N. Scherer, A. G. Schreyer and E. M. Jung, *Clin Hemorheol Microcirc*, 2010, **45**, 207-215.
3. D. Golovko, R. Meier, E. Rummeny and H. Daldrup-Link, *Int J Clin Rheumtol*, 2011, **6**, 67-75.
4. M. A. D'Agostino, E. A. Haavardsholm and C. J. van der Laken, *Best Pract Res Clin Rheumatol*, 2016, **30**, 586-607.
5. A. J. Greenup, B. Bressler and G. Rosenfeld, *Inflamm Bowel Dis*, 2016, **22**, 1246-1261.
6. O. C. Boerman, H. Rennen, W. J. Oyen and F. H. Corstens, *Semin Nucl Med*, 2001, **31**, 286-295.
7. H. J. Rennen, F. H. Corstens, W. J. Oyen and O. C. Boerman, *Q J Nucl Med*, 2001, **45**, 167-173.
8. H. J. Rennen, O. C. Boerman, W. J. Oyen and F. H. Corstens, *Eur J Nucl Med*, 2001, **28**, 241-252.
9. C. P. Bleeker-Rovers, O. C. Boerman, H. J. J. M. Rennen, F. H. M. Corstens and W. J. G. Oyen, *Current Pharmaceutical Design*, 2004, **10**, 2935-2950.
10. F. Gemmel, N. Dumarey and M. Welling, *Semin Nucl Med*, 2009, **39**, 11-26.
11. S. Navalkissoor, E. Nowosinska, G. Gnanasegaran and J. R. Buscombe, *Nucl Med Commun*, 2013, **34**, 283-290.
12. S. Basu, T. Chryssikos, S. Moghadam-Kia, H. Zhuang, D. A. Torigian and A. Alavi, *Semin Nucl Med*, 2009, **39**, 36-51.
13. S. Basu, H. Zhuang, D. A. Torigian, J. Rosenbaum, W. Chen and A. Alavi, *Semin Nucl Med*, 2009, **39**, 124-145.
14. C. Wu, F. Li, G. Niu and X. Chen, *Theranostics*, 2013, **3**, 448-466.
15. S. Hess, S. H. Hansson, K. T. Pedersen, S. Basu and P. F. Hoilund-Carlsen, *PET Clin*, 2014, **9**, 497-519.
16. T. J. Ruth, *J Nucl Med Technol*, 2014, **42**, 245-248.
17. Y. Ito, S. Okuyama, T. Awano, K. Takahashi, T. Sato and I. Kanno, *Radiology*, 1971, **101**, 355-362.
18. J. P. Lavender, J. Lowe, J. R. Barker, J. I. Burn and M. A. Chaudhri, *Br J Radiol*, 1971, **44**, 361-366.
19. V. Kumar, D. K. Boddeti, S. G. Evans and S. Angelides, *Curr Radiopharm*, 2012, **5**, 71-75.
20. S. B. Jensen, K. M. Nielsen, D. Mewis and J. Kaufmann, *Nucl Med Commun*, 2013, **34**, 806-812.
21. S. H. Yeh and M. D. Kriss, *J. Nucl. Med.*, 1967, **8**, 666-677.
22. P. B. Schneider, *J. Nucl. Med.*, 1973, **14**, 843-845.

23. L. J. Gati, L. I. Wiebe, J. W. Tse, C. J. Turner and A. A. Noujaim, *Nucl Med Biol*, 1986, **13**, 253-255.
24. T. P. Haynie, T. Konikowski and H. J. Glenn, *J. Nucl. Med.*, 1977, **18**, 915-918.
25. M. T. Ercan, T. Aras, I. S. Ünsal, Ü. Arıkan, E. Ünlenen and Z. Hasçelik, *Med J Islamic World Acad Sci*, 1992, **5**, 180-188.
26. M. T. Ercan, T. Aras, E. Unlenen, M. Unlu, I. S. Unsal and Z. Hascelik, *Nucl Med Biol*, 1993, **20**, 881-887.
27. Z. Wu, M. Liu, W. Lin and J. Feng, *Zhongguo Linchuang Kangfu*, 2004, **8**, 1553-1555.
28. M. T. Ercan and E. Unlenen, *Nucl Med Biol*, 1994, **21**, 143-149.
29. J. F. Chu, X. B. Wang, G. X. Lv, Y. Zhao, J. B. Zhang, J. C. Wang, H. Z. Mi and H. Yang, *J Radioanal Nucl Chem*, 2002, **254**, 397-400.
30. M. Caglar, A. M. Tokgozoglu, M. T. Ercan, T. Aras and C. F. Bekdik, *Clin Nucl Med*, 1995, **20**, 712-716.
31. A. Bhatnagar, P. Mishra, R. Sharma, K. Chuttani, K. Chakravarty, C. M. Jain, A. Mondal, M. K. Chopra and A. Gupta, *Nucl Med Commun*, 1999, **20**, 1067-1076.
32. R. Sharma, A. Mondal, A. Bhatnagar, K. L. Chakravarty, P. Mishra, M. K. Chopra, H. S. Rawat and R. Kashyap, *Clin Nucl Med*, 1998, **23**, 758-763.
33. M. T. Ercan, T. Aras, A. M. S. Aldahr, E. Unlenen, G. Mocan and C. F. Bekdik, *Nucl Med Commun*, 1993, **14**, 798-804.
34. C. Turan, A. Tutus, M. T. Ercan, B. H. Ozokutan, T. Yolcu, P. Kose and M. Kucukaydin, *Res Exp Med*, 1997, **197**, 157-164.
35. C. Turan, A. Tutus, B. H. Ozokutan, T. Yolcu, O. Kose and M. Kucukaydin, *J Pediatr Surg*, 1999, **34**, 1272-1275.
36. N. C. M. Gulaldi, H. Bayhan, M. T. Ercan, M. Kibar, B. Ozturk, M. Ogretensoy and C. F. Bekdik, *Clin Nucl Med*, 1995, **20**, 1012-1014.
37. A. Bhatnagar, P. Mishra, A. K. Singh, V. Taneja, U. P. S. Chauhan and K. Sawroop, *Clin Nucl Med*, 1996, **21**, 685-688.
38. U. P. S. Chauhan, P. Mishra, K. Chuttani, A. Bhatnagar and C. S. Bal, *Nucl Med Commun*, 1996, **17**, 979-985.
39. K. Özker and İ. Urgancioĝlu, *Eur J Nucl Med*, 1981, **6**, 173-176.
40. M. T. Ercan, T. Aras and I. S. Unsal, *Nucl Med Biol*, 1992, **19**, 803-806.
41. K. E. Britton, S. Vinjamuri, A. V. Hall, K. Solanki, Q. H. Siraj, J. Bomanji and S. Das, *Eur J Nucl Med*, 1997, **24**, 553-556.
42. J. Lecina, P. Cortes, M. Llagostera, C. Piera and J. Suades, *Bioorg Med Chem*, 2014, **22**, 3262-3269.
43. A. K. Singh, J. Verma, A. Bhatnagar and A. Ali, *World J Nucl Med*, 2003, **2**, 103-109.
44. M. S. Akhtar, M. B. Imran, M. A. Nadeem and A. Shahid, *Int J Pept*, 2012, **2012**, 965238.
45. S. Auletta, F. Galli, C. Lauri, D. Martinelli, I. Santino and A. Signore, *Clin Transl Imaging*, 2016, **4**, 229-252.
46. K. E. Britton, D. W. Wareham, S. S. Das, K. K. Solanki, H. Amaral, A. Bhatnagar, A. H. Katamihardja, J. Malamitsi, H. M. Moustafa, V. E. Soroa, F. X. Sundram and A. K. Padhy, *J Clin Pathol*, 2002, **55**, 817-823.
47. K. K. Halder, D. K. Nayak, R. Baishya, B. R. Sarkar, S. Sinha, S. Ganguly and M. C. Debnath, *Metallomics*, 2011, **3**, 1041-1048.
48. C. Palestro, C. Love, R. Caprioli, S. Marwin, H. Richardson, J. Haight, G. Tronco, P. Pugliese and K. Bhargava, *J Nucl Med*, 2006, **47**, 152P.
49. M. A. Motaleb, *J Label Comp Radiopharm*, 2009, **52**, 415-418.
50. R. H. Siaens, H. J. Rennen, O. C. Boerman, R. Dierckx and G. Slegers, *J Nucl Med* 2004, **45**, 2088-2094.
51. D. K. Nayak, R. Baishya, K. K. Halder, T. Sen, B. R. Sarkar, S. Ganguly, M. K. Das and M. C. Debnath, *Metallomics*, 2012, **4**, 1197-1208.
52. M. A. Motaleb, *J Radioanal Nucl Chem*, 2007, **272**, 95-99.

53. E. A. El-Ghany, A. M. Amin, O. A. El-Kawy and M. Amin, *J Label Comp Radiopharm*, 2007, **50**, 25-31.
54. S. Zhang, W. Zhang, Y. Wang, Z. Jin, X. Wang, J. Zhang and Y. Zhang, *Bioconjugate Chem*, 2011, **22**, 369-375.
55. I. T. Ibrahim, M. A. Motaleb and K. M. Attalah, *J Radioanal Nucl Chem*, 2010, **285**, 431-436.
56. E. A. El-Ghany, M. T. El-Kolaly, A. M. Amine, A. S. El-Sayed and F. Abdel-Gelil, *J Radioanal Nucl Chem*, 2005, **266**, 131-139.
57. M. Erfani, A. Doroudi, L. Hadisi, A. Andishmand, S. F. Mirshojaei and M. Shafiei, *J Label Comp Radiopharm*, 2013, **56**, 627-631.
58. S. Chattopadhyay, S. Saha Das, S. Chandra, K. De, M. Mishra, B. Ranjan Sarkar, S. Sinha and S. Ganguly, *Appl Rad Isot*, 2010, **68**, 314-316.
59. S. Q. Shah, A. U. Khan and M. R. Khan, *Nuklearmedizin*, 2011, **50**, 134-140.
60. M. Erfani, M. Rekabgardan, P. Mortazavi and M. Shafiei, *J Radioanal Nucl Chem*, 2016, **308**, 825-833.
61. S. O. Diniz, C. F. Siqueria, D. L. Nelson, J. Martin-Comin and V. N. Cardoso, *Braz. Arch. Biol. Technol.*, 2005, **48(S)**, 89-96.
62. S. O. Diniz, C. M. Rezende, R. Serakides, R. L. Ferreira, T. G. Ribeiro, J. Martin-Comin and V. N. Cardoso, *Nucl Med Commun*, 2008, **29**, 830-836.
63. S. M. Ferreira, G. P. Domingos, S. Ferreira Ddos, T. G. Rocha, R. Serakides, C. M. de Faria Rezende, V. N. Cardoso, S. O. Fernandes and M. C. Oliveira, *Bioorg Med Chem Lett*, 2012, **22**, 4605-4608.
64. L. E. Teixeira, G. G. Soares, H. C. Teixeira, I. K. Takenaka, S. O. Diniz, M. A. de Andrade, V. N. Cardoso and I. D. de Araujo, *Surg Infect (Larchmt)*, 2015, **16**, 352-357.
65. P. H. Costa, S. O. Diniz, V. N. Cardoso, B. Tarabal, I. Takenaka, O. Braga, P. V. Vidigal, C. L. Gelape and I. D. Araujo, *Acta Cir Bras*, 2015, **30**, 632-638.
66. M. A. Motaleb, *J Radioanal Nucl Chem*, 2007, **272**, 167-171.
67. M. Mostafa, M. A. Motaleb and T. M. Sakr, *Appl Rad Isot*, 2010, **68**, 1959-1963.
68. S. Chattopadhyay, M. Ghosh, S. Sett, M. K. Das, S. Chandra, K. De, M. Mishra, S. Sinha, B. Ranjan Sarkar and S. Ganguly, *Appl Rad Isot*, 2012, **70**, 2384-2387.
69. F. Y. Lambrecht, K. Durkan and P. Unak, *J Radioanal Nucl Chem*, 2008, **275**, 161-164.
70. F. Y. Lambrecht, O. Yilmaz, P. Unak, B. Seyitoglu, K. Durkan and H. Baskan, *J Radioanal Nucl Chem*, 2008, **277**, 491-494.
71. M. Sohaib, Z. Khurshid and S. Roohi, *J Label Comp Radiopharm*, 2014, **57**, 652-657.
72. A. Kaul, P. P. Hazari, H. Rawat, B. Singh, T. C. Kalawat, S. Sharma, A. K. Babbar and A. K. Mishra, *Int J Infect Dis*, 2013, **17**, e263-270.
73. N. Singh and A. Bhatnagar, *Tuberc Res Treat*, 2010, **2010**, 618051.
74. A. Samad, Y. Sultana, R. K. Khar, M. Aqil, M. A. Kalam, K. Chuttani and A. K. Mishra, *J Drug Target*, 2008, **16**, 509-515.
75. S. Roohi, A. Mushtaq and S. A. Malik, *Radiochim Acta*, 2005, **93**, 415-418.
76. A. Vito, H. Alarabi, S. Czorny, O. Beiraghi, J. Kent, N. Janzen, A. R. Genady, S. A. Alkarmi, S. Rathmann, Z. Naperstkow, M. Blacker, L. Llano, P. J. Berti and J. F. Valliant, *PloS one*, 2016, **11**, e0167425.
77. S. Hina, M. I. Rajoka, S. Roohi, A. Haque and M. Qasim, *Applied Biochemistry and Biotechnology*, 2014, **174**, 1420-1433.
78. D. Ilem-Ozdemir, M. Asikoglu, H. Ozkilic, F. Yilmaz, M. Hosgor-Limoncu and S. Ayhan, *J Label Comp Radiopharm*, 2014, **57**, 36-41.
79. S. K. Shahzadi, M. A. Qadir, S. Shabnam and M. Javed, *Arabian Journal of Chemistry*, 2015, DOI: 10.1016/j.arabjc.2015.04.003.
80. M. A. Motaleb, M. T. El-Kolaly, A. B. Ibrahim and A. Abd El-Bary, *J Radioanal Nucl Chem*, 2011, **289**, 57-65.
81. C. Tsopelas, S. Penglis and F. D. Bartholomeusz, *Nucl Med Rev Cent East Eur*, 2002, **5**, 93-97.

82. C. Tsopelas, S. Penglis, A. Ruszkiewicz and F. D. L. Bartholomeusz, *Nucl Med Biol*, 2003, **30**, 169-175.
83. D. Baldoni, R. Waibel, P. Blauenstein, F. Galli, V. Iodice, A. Signore, R. Schibli and A. Trampuz, *Mol Imaging Biol*, 2015, **17**, 829-837.
84. A. Lupetti, M. M. Welling, U. Mazzi, P. H. Nibbering and E. K. J. Pauwels, *Eur J Nucl Med Mol Imaging*, 2002, **29**, 674-679.
85. A. Lupetti, M. M. Welling, E. K. J. Pauwels and P. H. Nibbering, *Curr Drug Targets*, 2005, **6**, 945-954.
86. D. N. de Assis, V. C. Mosqueira, J. M. Vilela, M. S. Andrade and V. N. Cardoso, *Int J Pharm*, 2008, **349**, 152-160.
87. A. L. Reyes, L. Fernandez, A. Rey and M. Teran, *Curr Radiopharm*, 2014, **7**, 144-150.
88. R. Siaens, V. G. Eijsink, G. Vaaje-Kolstad, K. Vandenbulcke, B. Cornelissen, C. Cuvelier, R. Dierckx and G. Slegers, *Q J Nucl Med Mol Imaging*, 2006, **50**, 155-166.
89. Y. Z. Wang, L. Chen, X. R. Liu, D. F. Cheng, G. Z. Liu, Y. X. Liu, S. P. Dou, D. J. Hnatowich and M. Rusckowski, *Nucl Med Biol*, 2013, **40**, 89-96.
90. A. Lupetti, M. G. de Boer, P. Erba, M. Campa and P. H. Nibbering, *Med Mycol*, 2011, **49** Suppl 1, S62-69.
91. M. M. Welling, P. H. Nibbering, A. Paulusma-Annema, P. S. Hiemstra, E. K. Pauwels and W. Calame, *J Nucl Med*, 1999, **40**, 2073-2080.
92. M. Chianelli, O. C. Boerman, G. Malviya, F. Galli, W. J. G. Oyen and A. Signore, *Curr Pharm Des*, 2008, **14**, 3316-3325.
93. A. Lupetti, M. M. Welling, E. K. Pauwels and P. H. Nibbering, *Lancet Infect Dis*, 2003, **3**, 223-229.
94. M. S. Akhtar, J. Iqbal, M. A. Khan, J. Irfanullah, M. Jehangir, B. Khan, I. Ul-Haq, G. Muhammad, M. A. Nadeem, M. S. Afzal and M. B. Imran, *J Nucl Med*, 2004, **45**, 849-856.
95. M. M. Welling, S. Mongera, A. Lupetti, H. S. Balter, V. Bonetto, U. Mazzi, E. K. Pauwels and P. H. Nibbering, *Nucl Med Biol*, 2002, **29**, 413-422.
96. L. Melendez-Alafort, M. Ramirez Fde, G. Ferro-Flores, C. Arteaga de Murphy, M. Pedraza-Lopez and D. J. Hnatowich, *Nucl Med Biol*, 2003, **30**, 605-615.
97. L. Melendez-Alafort, A. Nadali, G. Pasut, E. Zangoni, R. De Caro, L. Cariolato, M. C. Giron, I. Castagliuolo, F. M. Veronese and U. Mazzi, *Nucl Med Biol*, 2009, **36**, 57-64.
98. G. Ferro-Flores, C. Arteaga de Murphy, M. Pedraza-Lopez, L. Melendez-Alafort, Y. M. Zhang, M. Rusckowski and D. J. Hnatowich, *Nucl Med Biol*, 2003, **30**, 597-603.
99. P. H. Nibbering, M. M. Welling, A. Paulusma-Annema, C. P. Brouwer, A. Lupetti and E. K. Pauwels, *J Nucl Med*, 2004, **45**, 321-326.
100. M. S. Akhtar, M. E. Khan, B. Khan, J. Irfanullah, M. S. Afzal, M. A. Khan, M. A. Nadeem, M. Jehangir and M. B. Imran, *Eur J Nucl Med Mol Imaging*, 2008, **35**, 1056-1064.
101. L. Melendez-Alafort, J. Rodriguez-Cortes, G. Ferro-Flores, C. Arteaga De Murphy, R. Herrera-Rodriguez, E. Mitsoura and C. Martinez-Duncker, *Nucl Med Biol*, 2004, **31**, 373-379.
102. M. S. Akhtar, A. Qaisar, J. Irfanullah, J. Iqbal, B. Khan, M. Jehangir, M. A. Nadeem, M. A. Khan, M. S. Afzal, I. Ul-Haq and M. B. Imran, *J. Nucl Med*, 2005, **46**, 567-573.
103. E. Vallejo, I. Martinez, A. Tejero, S. Hernandez, L. Jimenez, D. Bialostozky, G. Sanchez, H. Ilarraza and G. Ferro-Flores, *Arch Med Res*, 2008, **39**, 768-774.
104. L. Sarda-Mantel, A. Saleh-Mghir, M. M. Welling, A. Meulemans, J. M. Vrigneaud, O. Raguin, F. Hervatin, G. Martet, F. Chau, R. Lebtahi and D. Le Guludec, *Eur J Nucl Med Mol Imaging*, 2007, **34**, 1302-1309.
105. M. Gandomkar, R. Najafi, M. Shafiei, M. Mazidi, M. Goudarzi, S. H. Mirfallah, F. Ebrahimi, H. R. Heydarpor and N. Abdie, *Nucl Med Biol*, 2009, **36**, 199-205.
106. A. Fard-Esfahani, D. Beiki, B. Fallahi, M. R. Mohajeri-Tehrani, M. R. Gharaie, N. Rouhipour, M. Dehghanian, M. Saghari, A. Emami-Ardekani and M. Eftekhari, *Iran J Nucl Med*, 2010, **18**, 20-28.

107. M. Assadi, K. Vahdat, I. Nabipour, M. R. Sehhat, F. Hadavand, H. Javadi, A. Tavakoli, J. Saberifard, M. R. Kalantarhormozi, A. Zakani and M. Eftekhari, *Nucl Med Commun*, 2011, **32**, 716-723.
108. B. Nazari, Z. Azizmohammadi, M. Rajaei, M. Karami, H. Javadi, M. Assadi and I. N. Asli, *Nucl Med Commun*, 2011, **32**, 745-751.
109. D. Beiki, G. Yousefi, B. Fallahi, M. N. Tahmasebi, A. Gholamtezanezhad, A. Fard-Esfahani, M. Efani and M. Eftekhari, *Iran J Pharm Res*, 2013, **12**, 347-353.
110. A. A. Esmailiejah, M. Abbasian, S. Azarsina, F. Safdari, M. Amoui and S. Hosseinzadeh, *Arch Iran Med*, 2015, **18**, 371-375.
111. C. Arjun, A. Mukherjee, J. Bhatt, P. Chaudhari, K. M. Repaka, M. Venkatesh and G. Samuel, *Appl Rad Isot*, 2016, **107**, 8-12.
112. D. Salber, J. Gunawan, K. J. Langen, E. Fricke, P. Klauth, W. Burchert and S. Zijlstra, *J Nucl Med*, 2008, **49**, 995-999.
113. O. Tietz, A. Marshall, M. Wang and F. Wuest, *Curr. Med. Chem.*, 2013, **20**, 4350-4369.
114. M. Laube, T. Kniess and J. Pietzsch, *Molecules*, 2013, **18**, 6311-6355.
115. A. A. van Sorge, R. J. van Etten, C. J. Rehmann, T. J. M. Rijnders and N. J. van Haeringen, *J Ocul Pharmacol Ther*, 2002, **18**, 185-195.
116. D. J. Yang, J. Bryant, J. Y. Chang, R. Mendez, C. S. Oh, D. F. Yu, M. Ito, A. Azhdarinia, S. Kohanim, E. Edmund Kim, E. Lin and D. A. Podoloff, *Anticancer Drugs*, 2004, **15**, 255-263.
117. M. Erfani, S. Sharifzadeh, A. Doroudi and M. Shafiei, *J Label Comp Radiopharm*, 2016, **59**, 284-290.
118. H. Thakkar, R. K. Sharma, A. K. Mishra, K. Chuttani and R. R. Murthy, *Aaps Pharmscitech*, 2005, **6**.
119. N. Farouk, M. El-Tawoosy, S. Ayoub and A. S. El-Bayoumy, *J Radioanal Nucl Chem*, 2011, **290**, 685-690.
120. V. D. Chadha, P. Iaird, G. Jan and A. A. Khan, *Austin J Nucl Med Radiother*, 2015, **2**, 1010.
121. F. J. Blanco, R. Guitian, J. Moreno, F. J. de Toro and F. Galdo, *J Rheumatol*, 1999, **26**, 1366-1373.
122. M. H. Sanad and A. M. Amin, *Radiochemistry*, 2013, **55**, 521-526.
123. E. A. El-Ghany, A. M. Amine, A. S. Ei-Sayed, M. T. El-Kolaly and F. Abdel-Gelil, *J Radioanal Nucl Chem*, 2005, **266**, 125-130.
124. M. R. Yadav, V. P. Pawar, S. M. Marvaniya, P. K. Halen, R. Giridhar and A. K. Mishra, *Bioorg Med Chem*, 2008, **16**, 9443-9449.
125. M. El-Tawoosy, A. F. Mahmoud and S. E. Soliman, *Radiochemistry*, 2014, **56**, 622-627.
126. M. A. Reiley, B. M. Silber, J. Medina, F. Kayser and W. D. Shrader, *Journal*, 2015, **US 2015/0374858**.
127. N. Ghosh, R. Chaki, V. Mandal and S. C. Mandal, *Pharmacol. Rep.*, 2010, **62**, 233-244.
128. D. Wang and R. N. Dubois, *Nature Rev Cancer*, 2010, **10**, 181-193.